Experimental Eye Research 150 (2016) 62–70

Contents lists available at ScienceDirect

Experimental Eye Research

journal homepage: www.elsevier.com/locate/yexer

Research article

Müller cell metabolic chaos during retinal degeneration

Rebecca L. Pfeiffer [a, b, *], Robert E. Marc [a, b], Mineo Kondo [c], Hiroko Terasaki [d], Bryan W. Jones [a, b]

[a] Dept of Ophthalmology, Moran Eye Center, University of Utah, Salt Lake City, UT, USA
[b] Interdepartmental Program in Neuroscience, University of Utah, Salt Lake City, UT, USA
[c] Department of Ophthalmology, Mie University Graduate School of Medicine, Tsu, Japan
[d] Department of Ophthalmology, Nagoya University, Graduate School of Medicine, Nagoya, Japan

ARTICLE INFO

Article history:
Received 1 October 2015
Received in revised form
21 April 2016
Accepted in revised form 25 April 2016
Available online 30 April 2016

Keywords:
Retinal degeneration
Müller cell
Retinal remodeling
Retina
Computational molecular phenotyping (CMP)
Retinitis pigmentosa (RP)

ABSTRACT

Müller cells play a critical role in retinal metabolism and are among the first cells to demonstrate metabolic changes in retinal stress or disease. The timing, extent, regulation, and impacts of these changes are not yet known. We evaluated metabolic phenotypes of Müller cells in the degenerating retina.

Retinas harvested from wild-type (WT) and rhodopsin Tg P347L rabbits were fixed in mixed aldehydes and resin embedded for computational molecular phenotyping (CMP). CMP facilitates small molecule fingerprinting of every cell in the retina, allowing evaluation of metabolite levels in single cells.

CMP revealed signature variations in metabolite levels across Müller cells from TgP347L retina. In brief, neighboring Müller cells demonstrated variability in taurine, glutamate, glutamine, glutathione, glutamine synthetase (GS), and CRALBP. This variability showed no correlation across metabolites, implying the changes are functionally chaotic rather than simply heterogeneous. The inability of any clustering algorithm to classify Müller cell as a single class in the TgP347L retina is a formal proof of metabolic variability in the present in degenerating retina.

Although retinal degeneration is certainly the trigger, Müller cell metabolic alterations are not a coherent response to the microenvironment. And while GS is believed to be the primary enzyme responsible for the conversion of glutamate to glutamine in the retina, alternative pathways appear to be unmasked in degenerating retina. Somehow, long term remodeling involves loss of Müller cell coordination and identity, which has negative implications for therapeutic interventions that target neurons alone.

1. Introduction

1.1. Retinal degeneration and remodeling

Retinal degenerations such as Usher Syndrome, retinitis pigmentosa (RP), and age-related macular degeneration (AMD) cause irreversible vision impairment. These disorders ultimately cause the death of all photoreceptors in large retinal areas, often triggered by rod degeneration. During and following photoreceptor degeneration, the neural retina undergoes progressive remodeling, including ectopic neuritogenesis, microneuroma formation, loss of distinct layer lamination, Müller cell hypertrophy, metabolic alterations of neurons and glia, and progressive neuronal loss (Kolb and Gouras, 1974; Strettoi et al., 2002; Fisher and Lewis, 2003; Jones et al., 2003; Marc and Jones, 2003; Marc et al., 2003; Strettoi et al., 2003; Jones and Marc, 2005; Jones et al., 2005, 2011, 2012).

Abbreviations: adRP, autosomal dominant retinitis pigmentosa; AMD, age-related macular degeneration; CDF, cumulative distribution function; CMP, computational molecular phenotyping; CRALBP, cellular Retinaldehyde binding protein 1; EAAT, excitatory amino acid transporter; GABA, γ-aminobutyric acid; GFAP, glial fibrillary acidic protein; GS, glutamine synthetase; KS test, Kolmogorov-Smirnov test; mdCMP, morphology driven CMP; RPE, retinal pigmented epithelium; RP, retinitis pigmentosa; rgb, red green blue; SNAT, sodium-coupled neutral amino acid transporter; Tg P347L, rabbit rhodopsin proline 347 → leucine transgenic model of autosomal dominant RP.

* Corresponding author. University of Utah, Moran Eye Center, 65 Mario Capecchi, Dr., Salt Lake City, UT 84132, USA.
E-mail address: R.Pfeiffer@utah.edu (R.L. Pfeiffer).

http://dx.doi.org/10.1016/j.exer.2016.04.022

The mechanisms of these alterations are not fully characterized and their impacts on the long-term viability of therapeutic interventions are uncertain (Marc et al., 2014).

1.2. Müller glia in degenerating retina

Müller glia are among the first to show metabolic changes in retinal degenerations. Müller cells support many neuronal metabolic processes including (but not limited to) glucose transport, removal of NH_3^+ byproducts, CO_2, redistribution of K^+, and recycling amino acids (Newman et al., 1984; Wilson, 2002; Reichenbach and Bringmann, 2010; Bringmann et al., 2013; Hurley et al., 2015). Müller cell morphology varies subtly between aerobic and anaerobic retinas, but no major functional differences in metabolic support have been described (Dreher et al., 1992), except for the absence of GABA transport and recycling in non-mammalians (Marc, 1992, 2004). Müller cells are thought to be a homogenous class in all vertebrates. Though there has been some indication of Müller cell heterogeneity based on previous genetic and cell culture experiments, functional and metabolic subclasses have never been observed (Rowan and Cepko, 2004; Roesch et al., 2012). Müller cells display a characteristic normal small molecule signature high in taurine and glutamine and very low in all other markers including glutamate across all vertebrate classes (Marc, 2004). Indeed these signatures are indistinguishable despite vast differences in systemic biology across vertebrates, including avascular ectotherms such as teleost fishes (Marc et al., 1995; Marc and Cameron, 2001), avascular non-mammalian endotherms such as avians (Kalloniatis and Fletcher, 1993), avascular mammals (Marc, 1992), and a range of vascular mammals such as mouse, rat, cat, and primate (Kalloniatis et al., 1996; Jones et al., 2003; Marc et al., 1998a,b, 2008). Mammalian Müller cells display a definitive protein signature with elevated glutamine synthetase (GS) and cytosolic retinaldehyde binding protein (CRALBP) and respond to stress (e.g. reactive oxygen species stress) with massive upregulation of glial fibrillary acidic protein (GFAP) levels (Bignami and Dahl, 1979; Erickson et al., 1987; Fisher and Lewis, 2003; Luna et al., 2010).

1.3. Müller glia functions and homogeneity

Müller cells are thought to be an essential component of glutamate recycling in the retina (Pow and Robinson, 1994) by importing extracellular glutamate via high-affinity Na^+-dependent transporters (e.g. EAAT1) and rapidly amidating it to glutamine via GS (Riepe and Norenburg, 1977). Müller cells then export glutamine via a Na^+-dependent transporter (SNAT3) into the extracellular compartment where neurons can import it via SNAT1 and other mechanisms for synthesis of neurotransmitters and other metabolites. Due to rapid amidation by GS, glutamate is only found at $\approx$0.1–0.6 mM in Müller cells, in contrast to bipolar or ganglion cells where it may be as high as 10 mM (Marc et al., 1990; Marc and Jones, 2002; Marc, 2004). Retinal glutamate synthesis is commonly thought to be predominantly dependent on the glutamine/glutamate cycle (Marc, 2004) and, therefore, GS activity (Pow and Robinson, 1994). It has been presumed, that the homogeneity of Müller cell metabolic signatures is shaped by the microenvironment created by neurons surrounding the Müller column, including cone photoreceptors (Reichenbach and Bringmann, 2010). Data from previous work in our lab (Jones et al., 2011) and the results presented here indicate this may not be the case.

1.4. Transgenic P347L rabbit model of autosomal-dominant retinitis pigmentosa (adRP)

Numerous animal models have been developed for studying retinitis pigmentosa, including fruit fly (Griciuc et al., 2012; Chow et al., 2016), zebrafish (Brockerhoff et al., 1995), mouse (Keeler, 1924; Pittler et al., 1993; Chang et al., 2002; Han et al., 2013), rat (Bourne et al., 1938), chicken (Semple-Rowland and Lee, 2000), pig (Petters et al., 1997), cat (Narfstrom, 1983; Barnett and Curtis, 1985), and dog (Aguirre, 1978; Suber et al., 1993). Of these animal models, the large eye models have proven to be especially useful for analyzing retinal degenerations (Jones et al., 2011) and testing new treatments (Chader, 2002), though larger animals can be expensive, slow to mature and breed. To address this problem a transgenic rabbit model with a primary rod degeneration caused by a human rhodopsin proline 347 → leucine mutation characteristic of a human variant of adRP was developed by the Kondo laboratory (Kondo et al., 2009). We have previously characterized the progression of degeneration in this rabbit model over the first year of degeneration, demonstrating that it progresses through cone-sparing retinal degeneration analogous to that seen in humans. In brief, the degeneration presents initially with loss of rod photoreceptors, which may survive up to 12–16 weeks; subsequently, cone photoreceptors will also degenerate by around 40 weeks of age. During this time the neural retina becomes deafferented and undergoes a series of remodeling events including massive rewiring through microneuromas, changes in cell types and numbers, and Müller cell hypertrophy and metabolic changes. For a more comprehensive description of the remodeling associated with this model see previous publications (Jones et al., 2011, 2012).

1.5. Computational molecular phenotyping

This study focuses on the metabolic changes in Müller cells during degeneration and quantifies the changes across Müller cells as a class and within individual cells. The technique used for this study is computational molecular phenotyping (CMP), which allows for quantitative evaluation of metabolite levels within single cells (Marc et al., 1995; Kalloniatis et al., 1996; Marc and Cameron, 2001). This is unique to our approach as it obviates dissociation and/or homogenization required for biochemical assays and uniquely allows visualization of metabolic diversity. Indeed, the key finding enabled by CMP is that Müller cells in degenerating retinas slowly lose the ability to uniformly regulate their metabolomes.

2. Methods

2.1. Model systems

The heterozygous Transgenic (Tg) P347L rabbit is a model of human adRP, originally generated in the Kondo laboratory (Kondo et al., 2009). In brief, these rabbits express a mutated rhodopsin gene with a C-to-T transition at proline 347, causing a proline to leucine replacement. This mutation causes degeneration of the photoreceptors phenotypically similar to other adRP mutations and to human cone-sparing RP (Jones et al., 2011). Control rabbits used in these experiments are the transgene negative unaffected littermates of the TgP347L rabbits (WT). Two TgP347L rabbits, ages 2 years and 2 years 5 months, were selected to evaluate late stage adRP degenerating retina. Two WT rabbits were selected for illustrative comparison ($\approx$6–12 months and 3 year 8 month rabbit). For additional statistical analysis, we compared these to Müller cell datasets from diverse vertebrates in our library including samples from 150 goldfish; 13 primates; 65 rats including 25 with fetal retinal transplants and 30 from early phase retinal degenerations that show no Müller cell changes; and over 1450 separate assays from 90 rabbits, most 6–12 months old but some as old as 2 years. We also have very aged human samples that show no Müller cell variations (Jones et al., 2016a, 2016b). In total we have at least 559

retinal samples from 319 individual animals.

2.2. Tissue processing

Retinal samples were harvested as previously described (Marc et al., 1990; Marc, 1999). Rabbits were tranquilized with intramuscular ketamine/xylazine followed by deep anesthesia with 2-3 doses of 15% aqueous intraperitoneal urethane, followed by bilateral thoracotomy. All animal experiments were conducted according to the ARVO Statement for the Use of Animals in Ophthalmic and Vision Research, with the approval of the Institutional Animal Care and Use Committee at the University of Utah. Following euthanasia, both eyes were removed and hemisected. Retinas were cut into smaller pieces and placed in 2.5% glutaraldehyde, 1% formaldehyde, 0.1 M cacodylate (pH 7.4), 1 mM $MgSO_4$, 3% sucrose fixation solution. After 24 h fixation, tissues were dehydrated through graded methanols to acetone and embedded in an epoxide resin (Marc et al., 1995). Tissue stacks (Marc et al., 1990) were serially sectioned at 100 nm onto 12-well array slides.

2.3. CMP and nomenclature

We used CMP to identify cell classes and quantify the effects of retinal degeneration on core retinal metabolism (Marc et al., 1995; Marc and Cameron, 2001; Jones et al., 2003). Each well of the array slide was probed with an IgG selective for one of seven small molecules denoted by single letter codes as described in previous publications (D aspartate, E glutamate, G glycine, J glutathione, Q glutamine, τ taurine, γ GABA), CRALBP, or GS and visualized with a secondary antibody conjugated to a 1.4 nm gold granule, followed by silver intensification (Marc et al., 1995; Marc and Jones, 2002) (Table 1). CMP yields quantitative measures of small molecules, enables computational classification of cells, and defines a signature for each class. When we refer to a molecule's signal, we will use protein amino acid notation, e.g. E for glutamate (Marc et al., 1995). A triplet mapping refers to the assignment of a molecule to a color channel, e.g. γGE → rgb (Marc and Cameron, 2001). Finally, a signature refers to the pattern of signal strengths associated with set of molecules that define a cell class (Marc and Jones, 2002) and can be several molecules long depending on the number of channels we use. But in practice, Müller cells are defined by a four-channel signature with high taurine and glutamine (τ^+ and Q^+), moderate glutathione levels J, and low glutamate we denote by E^0. Normal Müller cells also have very low alanine, arginine, aspartate, glycine and GABA levels (Marc et al., 1995, 1998a,b). Thus when we refer to the Müller cell "τQE" signature, we imply the $\tau^+Q^+JE^0$ complex signature.

2.4. Analysis

We used K-means clustering (Marc et al., 1995) to identify all natural cellular compartments, all molecular signals were captured as 8 bit images using a cooled QImaging Retiga CCD camera (Surrey, BC) under constant gain and flux. The channels were then computationally aligned using ir-tweak (Anderson et al., 2009), generating a registered volume of individual grayscale images of each metabolite. To generate a cluster theme map all channels were loaded into custom software (CMP, Scientific Computing Institute, Salt Lake City UT), which facilitated k-means clustering with a masking option to remove background and kerf. This classification was run iteratively with k increased by 1 until it converged on statistics consistent with known biological classes (Marc et al., 1995). From these data, we can determine absolute metabolite levels in all cell classes, visualized as univariate histograms (CellKit, © Robert E. Marc, 2003).

Due to the high variability in Müller cell signals observed in late phase III advanced phases of retinal degeneration, a modified classification was developed. Sections were clustered using the same K-means classification as in normal retina, but this yielded many different classes for individual Müller cells across the retina. We grouped the Müller cell subclasses into a single artificial class by metabolic exclusion of neurons (e.g. subtraction of γ+, G+ or E+ neurons) and summation of remaining subclasses until they matched the morphology of Müller cells as defined by unique signals such as GS, τQE, and CRALBP in normal retina. This means of clustering is morphology-driven computational metabolic phenotyping (mdCMP). Finally, we used both binomial probability calculations and the single-sample methods of Crawford and Howell (1998) and Crawford and Garthwaite (2012) to determine population significances.

Image J (Schneider et al., 2012) and CellKit were used for histogram visualization, Microsoft Excel was used for cumulative distribution function (CDF) generation and statistical tests (e.g. Kolmogorov-Smirnov, KS), and Adobe Photoshop was used for final image creation. For ease of visualization of metabolite signals, channels are mapped to rgb images: τ, GS γ → red; Q and G → green; and E → blue. Thus a triplet of metabolites is mapped, for example, as γGE → rgb. The displayed images are max-min linearly stretched for human visualization. All statistics, clustering, and metabolic quantification were run on raw image data.

3. Results

During late stage (phase III) remodeling of the Tg P347L retina, after the loss of the sensory retina and global remodeling has

Table 1
Immunocytochemistry reagents.

Reagent	SKU	RRID	Source	Dilution
anti-L-alanine IgG	A100R	AB_2532052	Signature Immunologics	1:100
anti-agmatine IgG	B100R	AB_2532053	Signature Immunologics	1:100
anti-agmatine IgY	B100C	AB_2532054	Signature Immunologics	1:100
anti-L-aspartate IgG	D100R	AB_2341093	Signature Immunologics	1:100
anti-L-glutamate IgG	E100R	AB_2532055	Signature Immunologics	1:100
anti-L-glutamate IgY	E100C	AB_2532056	Signature Immunologics	1:100
anti-glycine IgG	G100R	AB_2532057	Signature Immunologics	1:100
anti-glutathione IgG	J100R	AB_2532058	Signature Immunologics	1:100
anti-L-glutamine IgG	Q100R	AB_2532059	Signature Immunologics	1:100
anti-taurine IgG	TT100R	AB_2532060	Signature Immunologics	1:100
anti-GABA IgG	YY100R	AB_2532061	Signature Immunologics	1:100
anti-GABA IgY	YY100C	AB_2532062	Signature Immunologics	1:100
anti-GS IgG	610517	AB_397879	BD Biosciences	1:50
anti-CRALBP IgG	NA	AB_2314227	Gift of Dr. Jack Saari	1:400

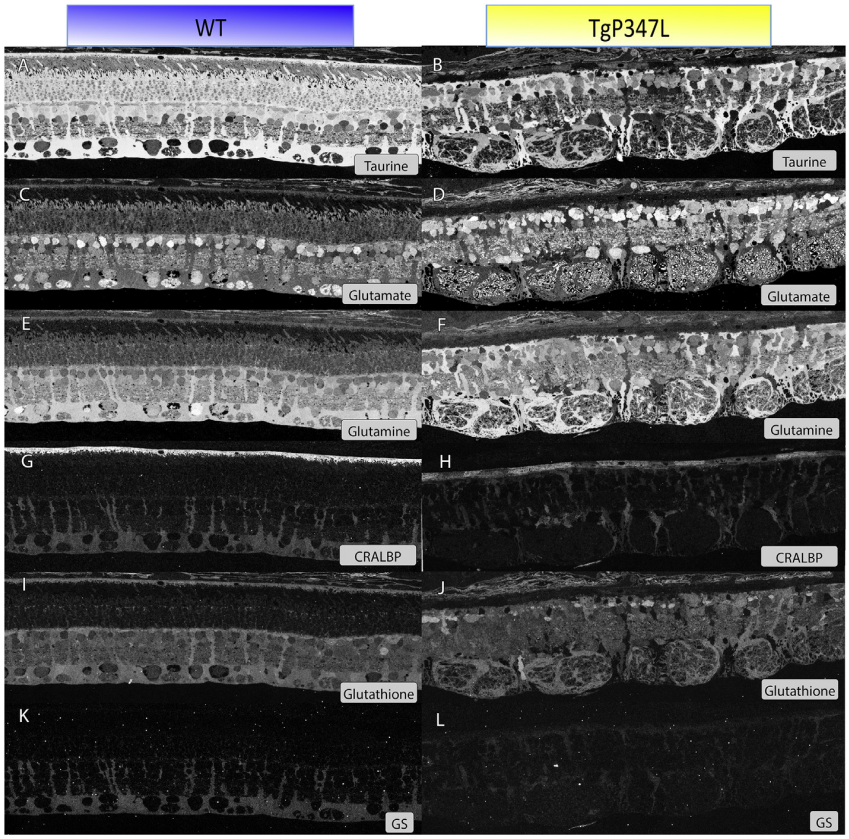

Fig. 1. Comparison of WT amino acid levels to that of Tg P347L. All images are the inverted silver density images of molecular immunoreactivity in serial 100 nm sections so that higher intensity = higher concentration. (Left) Registered WT small molecule channels. (Right) Registered TgP347L retina of the same channels as WT.

initiated (Marc et al., 2003; Jones et al., 2012), Müller cell metabolism changes more radically than we had ever seen. We sought to define the extent of metabolic variation in Müller cell small molecule and protein levels CMP examination of CMP signatures (Fig. 1), K-means clustering (Fig. 2) and quantitative histogramming (Fig. 3) and statistical analysis.

3.1. CMP signatures

During degeneration, Müller cell taurine content displays both dysregulation and intercellular variation in phase III remodeling (Fig. 1A,B). Some survivor Müller cells display higher taurine levels than normal while others display much lower levels. This variation is not regional, as vastly different Müller cells can be immediate neighbors. In contrast, glutamate (the core metabolite of neuronal signaling) appears to be quite high in survivor neurons and only slightly depressed in Müller cells (Fig. 1C,D). Given the near uniformity of glutamate signals in both WT and Tg P347L retinas, we expected a small uniform increase in Müller cell glutamine content as had been previously observed in retinal degenerations. But the phase III Tg P347L rabbit displays both strong glutamine elevation and as much intercellular variation as taurine (Fig. 1E,F). Another molecule linked to glutamate levels (as least as a sink for glutamate) is glutathione. In degenerate retina, the population mean of glutathione in Müller cells is similar to age-matched healthy controls, but intercellular levels are much more variable (Fig. 1I,J). Given these variations in small molecules, we explored whether characteristic protein markers of Müller cells were altered in any way. Even though CRALBP is not functionally linked to the glutamate-glutamine cycle, putative taurine osmoregulation, or the behavior of redox molecules like glutathione, CRALBP is also remarkably variable in remodeling Müller cells (Fig. 1G,H). The RPE of degenerating retina also has dramatically decreased and patchy CRALBP expression. Simultaneously, some Müller cells lack detectable CRALBP, while others upregulate content to match some remnant RPE cells. The high levels of CRALBP, in addition to similar levels of other metabolites, makes certain Müller cell metabolic signatures similar to RPE cells in remodeling. Finally, we see that GS is also severely reduced in phase III remodeling, but not uniformly. Like the other signatures, GS varies considerably between neighboring Müller cells in the same region of degenerate retina. But considering this change, it is also remarkable that Tg P347L rabbit glutamate signals in Müller cells rise above WT Müller cells in only a few instances, and even cells with low GS do not show large increases in glutamate content.

3.2. Clustering, histograms and analysis

The nature of Müller cell homogeneity in normal retina and variation the Tg P347L rabbit retina is far better visualized by combining single quantitative channels into classic τQE → rgb maps (Fig. 2A,C). Every Müller cell across the retina forms a single homogeneous class (Fig. 2A). By using all six channels to create a theme map of all statistically separable cell classes, it is easily demonstrated that a single class emerges for Müller cells (Fig. 2B). In normal retina, a τQE signature always separates the entire Müller

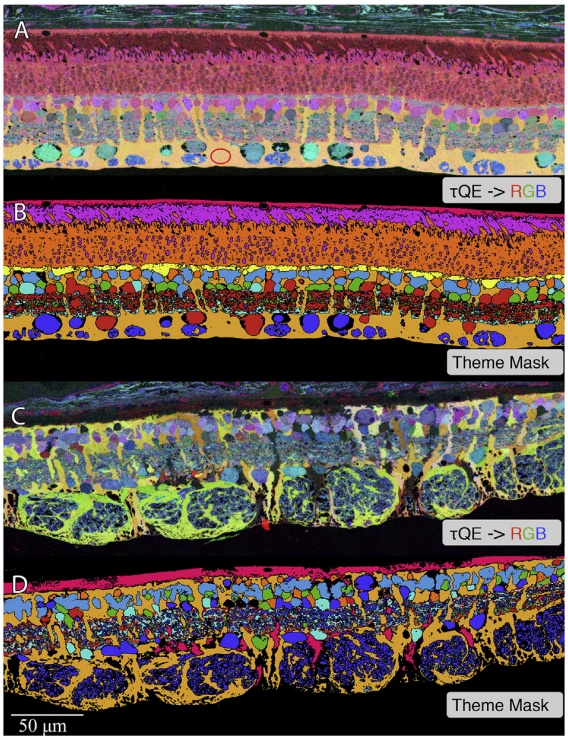

Fig. 2. Representative τQE and theme maps of WT retina vs degenerate retina. A and C are registered images of amino acid immunoreactivity in serial 100 nm sections. Both have been clustered using K-Means (k = 12) in which all classes of cells are separated by metabolic signature. Metabolic signatures used for generating maps: E,Q, J, τ, G, γ, GS, and CRALBP. 1A) τQE → rgb of a WT rabbit retina. The Müller cells (endfeet highlighted by red oval) are clearly identifiable by their characteristic shape and signature, which appears yellowish orange in this configuration. 1B) Clustering theme map of WT retina using 7 metabolic signatures. The orange theme class clearly identifies the Müller cells and makes them completely separable from all other cell types of the retina. 1C) τQE → rgb of TgP347L degenerate rabbit retina. The Müller cells have less pronounced endfeet in part due to hypertrophy that may include redistribution of volume from the endfeet to more apical locations within the retina. Müller cells display a range of colors. 1D) Theme map of the TgP347L retina. Simple K-means clustering does not extract Müller cells. By using the mCMP method the orange theme class was generated by fusing non-neuronal glial signatures into a single artificial class, demonstrating the location of the remaining Müller cells, with the exception of the pink group that has a signature metabolically similar to the RPE, due to a pronounced loss of typical Müller cell amino acids.

cell cohort from all other retinal cells. This is a formal proof, substantiated by direct measures, that metabolite levels and fluxes are highly conserved with low variance.

The Müller cell τQE signature of the phase III Tg P347L retina is an array of molecular mixtures. While variability is qualitatively evident in the τQE signature (Fig. 2C), the Müller cell cohort is proven to be inhomogenous when no clustering algorithm was capable of grouping all Müller cell variants into a class (not shown). But to provide a statistical test of the cohort as a whole, we had to fuse the many individual Müller cells into two major classes (Fig. 2D) as described in the methods.

Using the theme classes as a mask, we could then extract the histograms for normal and Tg P347L retinal Müller cells. In all cases, small molecule signals of Tg P347L rabbit Müller cells are much more variable than normal Müller cells (Fig. 3A–D). In addition, both proteins CRALBP and GS have essentially collapsed to very low levels (Fig. 3E,F).

How do we statistically assess individual Müller cell differences? First, the homogeneity in WT retina is so profound that borders between Müller cells are indistinguishable by optical microscopy. Using transmission electron microscope images from rabbit retinal connectome RC1 (Anderson et al., 2011) we evaluated the size of the endfeet of 301 neighboring Muller cells in the ganglion cell layer. This analysis revealed that the mean endfoot diameter is 5.2 ± 0.75 μm. By using a sampling area of 4 × 4 μm we ensured that each signal patch represents one or two (rarely three) Müller cells in WT retina. Horizontal sections through the endfeet of Müller cells in the ganglion cell layer were probed for τQE and their distributions evaluated for collections of individual Müller cells in WT and Tg retinas. The distributions were compared using a two-sample Kolmogorov-Smirnov (KS) test, which showed the distributions of the two populations were significantly different $p < 0.001$ (Fig. 4). It is obvious that from both the univariate histograms and the cumulative distribution functions (CFDs) that the variances of the Müller cell population sample in the Tg P347L retina are abnormally high.

To further stress that the variability is intercellular and not intracellular, we analyzed the CDFs of ten 4 × 4 μm samples, taken at separate locations to be indicative of separate Müller cells. These CDF's were compared to the normal distribution of the entire Müller cell population (Tg: ~817 Müller cells, WT: ~1053 Müller cells) in horizontal sections (Figs. 4 and 5). The CDFs from the individual endfeet in the WT section overlay closely with the total population indicating that there is low variability between individual cells and that they have consistent amino acid concentrations. In the Tg section, the CDF of the total population is much broader than the WT population and, remarkably, the CDFs from the endfeet of 10 individual remodeling Müller cells vary by as much as a log unit.

Finally, we have to address the problem of sample size. Rare clinical samples or expensive experiments that take long times to evolve are problematic but can be managed with classical combinatorial and parametric methods. First, while it is beyond the scope of this paper to produce hundreds of images, we nevertheless have τQE signatures for literally thousands of Müller cells from over a dozen species and hundreds of individual retinas and animals. All τQE signatures from non-mammalians and mammals are identical, except for very small shifts in amino acid means and all form a single class with extremely low variances (e.g. Marc et al., 1995, 1998a; Kalloniatis et al., 1996; Marc and Jones, 2003; etc.). All of these samples are archival and still exist in our libraries; they also include 2 year old rabbits, 27 year old macaques and a 78 year old human, all having the same single-class τQE signature. These older retinas are indistinguishable from juvenile retinas of any mammal. If we sample 100 Müller cells from each of 559 retinas and find only a single class, by clustering or visually, that sets the probability of success for repeating that conclusion in the next sample at no less than 0.9998. Using the binomial distribution one would argue that a sample from two Tg P347L rabbit retinas failing to form single Müller cell classes has a probability of 1×10^{-6}. This means that late phase III remodeling creates a state unlike any known retina and solves the rare case problem. More aggressively, we can use the approach developed for single-case research (Crawford and Howell, 1998; Crawford and Garthwaite, 2012) and use the histogram half-width of data from rabbit, goldfish and monkey as representative for the control half-width of all species. This has three important features. First, the half width is largely independent of the histogram mean. Second, we can pick the worst case data set based on the oldest cameras, noisiest immunocytochemistry and earliest technology (Marc et al., 1995) and show that newer histograms are narrower. Thus using the worst case control data biases against a type I error. Third, the half-width of each case is itself the average of many Müller cells, and so represents a measure of a single retina's variability. Using Marc et al. (1995) the half-width for the Müller

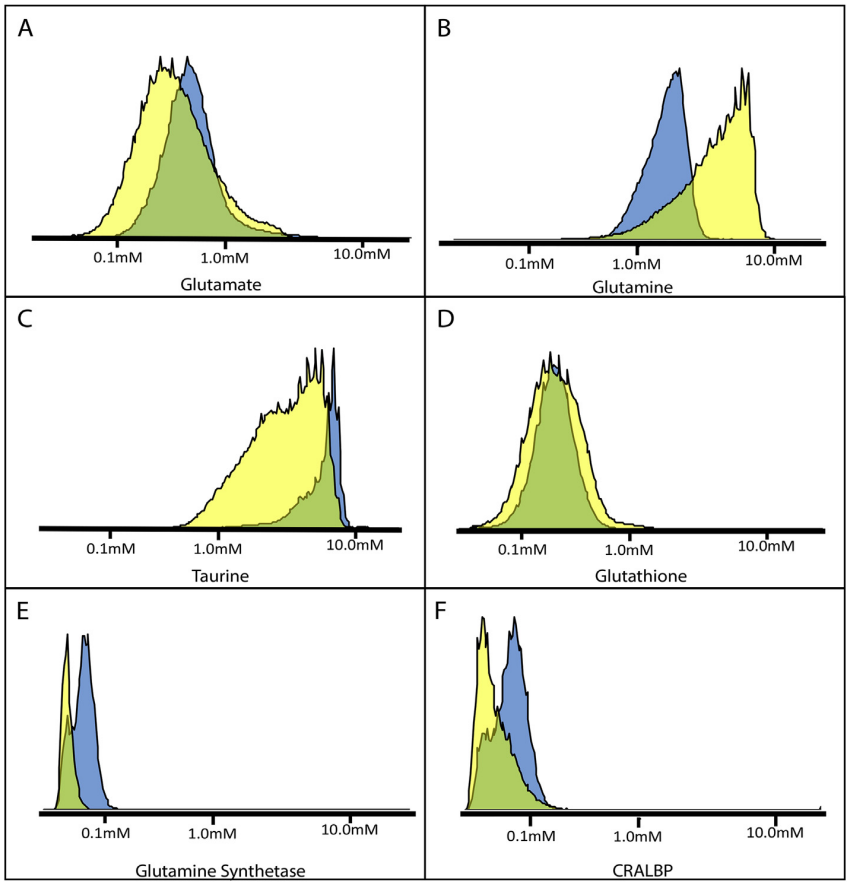

Fig. 3. Univariate amino acid probability density distributions (histograms) for each of the amino acids displayed in Fig. 2. (Yellow) Tg P347L retina; (Blue) WT retina. The histograms each represent aggregate signals from 15 to 20 Müller cells as described in Marc and Jones (Marc and Jones, 2002) and displayed as normalized probability density versus pixel values scaled as concentration.

cell taurine signal is 60 PV in an 8-bit image capture. Although the mean for taurine in the primate retina is lower than goldfish, the half-width is ≈50 PV. In the WT rabbit using low noise cameras, thinner sections and far better image registration the half-width is ≈PV 40. So we can safely assume that the mean half-width (x) is 50 PV or less with a range of 10 PV. If we conservatively call the range the standard deviation (s), and assume that the taurine half-width ($x_{tg} \approx 100$ PV) of the Tg P347L rabbit is the mean of an equivalent population, the formula for Student's $t_{n-1} = (x_{tg}-x)/(s \times (n + 1/n)^{1/2}) \geq 4$ over a range of n values and achieves $p < 0.01$ for any $n \geq 5$. So merely taking the three published half-widths and the two control widths shown here demonstrates that the rare outcome of these two Tg P347L rabbit retinas is not simply an outlier on the normal distribution.

4. Discussion

K-means clustering identifies all major cell classes and allows profiling of normal metabolite levels and variation in Müller cells of normal retina. The very fact that k-means fails to classify all Müller cells in the degenerating retina is a formal proof that Müller cell metabolism is highly variable in disease. We used mdCMP to reconstitute the entire Müller cell population and generated a theme map of cell types in the degenerate state (Fig. 2C–D).

This shows the metabolic revisions in retinal degenerations are more complex than previously believed. In every observed species, Müller cells show high homogeneity in their metabolic signatures in healthy retinas (Marc et al., 1990; Kalloniatis and Fletcher, 1993; Kalloniatis et al., 1996; Marc et al., 1998b; Marc and Cameron, 2001). However, in degenerating retina, Müller cells lose their remarkably precise metabolic homogeneity and become variable early in degeneration, with persistent changes throughout subsequent remodeling. It has been noted previously that much of the neural cell death and remodeling associated with photoreceptor loss can be delayed as long as cone photoreceptors are present, though other aspects of remodeling continue to occur (Jones et al., 2011, 2012). Previous publications also demonstrate that early in adRP degeneration, while cones are still present, Müller cells begin to slightly alter their metabolic signatures in respect to one another (Jones et al., 2011). We show that this early variability increases throughout later remodeling. If microenvironments shaped Müller cell signatures we would expect patchy signatures with neighboring Müller cells showing similar signatures. This never happens. Rather, signature variations appear to be independent of any geographic property. The variation appears more extensive in later stage remodeling retina than shown by Jones et al., 2011, further indicating a lack of predictability of metabolic variation during the course of adRP.

The probable impacts of these variations on retinal function are unclear, particularly as the mechanisms by which these alterations

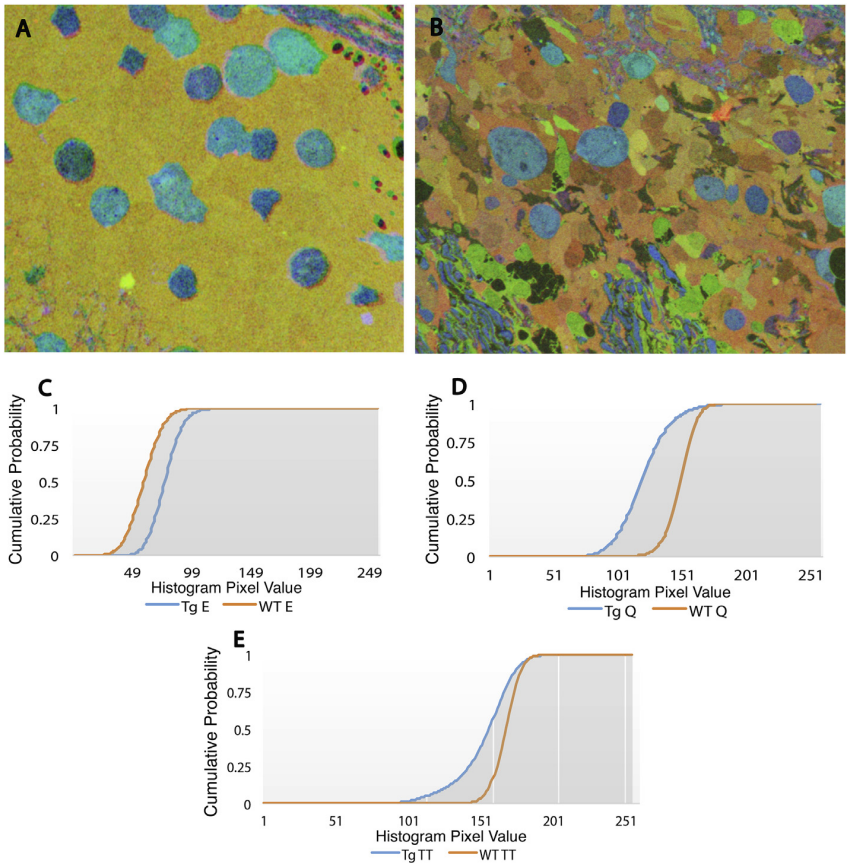

Fig. 4. 4A+B) τQE → rgb mappings of registered of amino acid signals in serial 100 nm sections. Color variation in an individual cells indicates varying differing ratios of τQE. (A) WT retina. (B) TgP347L retina C–E) Normal distributions of glutamate, glutamine, and taurine levels across entire Muller cell population of Tg P347L (blue) and WT retinas (red). All Tg distributions are significantly separable from WT distributions based on K-S test with a $p < 0.001$.

arise are unknown. Possible mechanisms and precipitating factors leading to the chaotic of signatures seen here in late stage remodeling retina will require further experimentation. These signatures may reflect transporter deficiencies of the Müller cells, unknown enzyme expression, or Müller cells entering altered cellular states reflecting division or progression towards cell death. One such striking altered mechanism is that the simple E → Q conversion by GS no longer defines Müller cell signatures. Remarkably, Müller cells appear to be able to both metabolize E and synthesize Q by yet unknown pathways. The nature of the signature variability is also unclear. It is possible that it is part of a common degeneration response pathway (which all Müller cells enter) where they are no longer synchronized with one another. This possibility will require the ability to track the changes in a group of cells over time. But the precision of normal Müller cell signatures is equally mysterious, as we know of no homeostatic synchronizer for cellular metabolism.

Extensive metabolic variation in remodeling retina is confounded by the fact that the changes do not follow patterns predicted by our current understanding of amino acid recycling. While the nonstoichiometric variation of E, Q, and GS is perplexing, it is not without possible explanation. It has been previously pointed out that GS is the not the only enzyme that uses E as a substrate, nor is there a known enzymatic cluster that exclusively controls E levels (Marc, 2004; McKenna, 2007). E is a primary carbon skeleton for a host of biochemical processes. A possible route for E metabolism in the absence of GS is the TCA cycle (Poitry et al., 2000). Previous studies in brain have shown that under acute increases in extracellular E (>200 μM) as much as 25% of extracellular E is metabolized via the TCA cycle generating lactate and aspartate (McKenna et al., 1996). This may provide a mechanism to supply energy demands of a pathologic system given the increase in the production of stress marker proteins (e.g. GFAP), Müller cell hypertrophy, and neuronal neuritegenesis. Other pathways that may explain the Q accumulation and E metabolism are alternate transaminases that could become expressed, activated or simply unmasked under conditions of degeneration (Michal, 1999; Reichenbach and Bringmann, 2010). One such aminotransferase is alanine aminotransferase (ALAT or ALT), which catalyzes the formation of alanine and alpha-ketoglutarate (αKG) from glutamate. These products combined with lactate may synthesize Q, either in the Müller cells, or may be transported to neurons as a precursor for glutamate. Further investigation into the accumulation of Q in some Müller cells, in the absence of GS, will be required.

The other signature characteristics observed in the late stage degenerating retina have numerous possible pathways and mechanisms by which they arise. One such mechanism is an alteration of taurine transport, because no cell of the neural retina synthesizes taurine (Marc et al., 1998b). Since the outer retina collapses in retinal remodeling with the ultimate emergence of a glial seal between the neural retina and any remaining RPE cells (Jones and Marc, 2005; Jones et al., 2011), it may be that some Müller cells

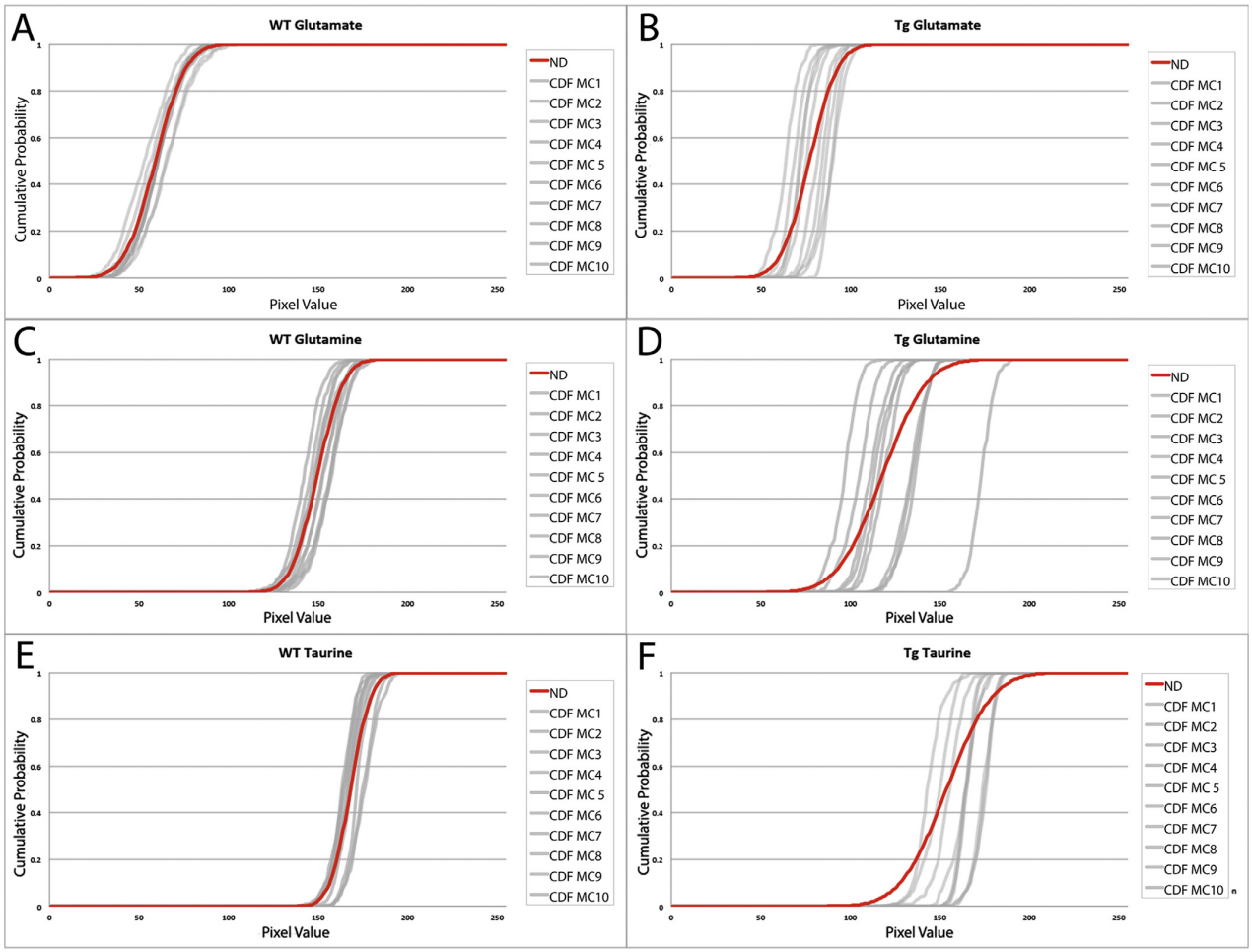

Fig. 5. Cumulative distribution frequencies (CDFs) of the entire Müller cell cohorts in the regions displayed in 4C–F (red Normal Distribution (ND) line) in addition to 10 4 × 4 μm regions from WT and degenerate retina (MC1-10 CDFs) as gray lines. On the left is the WT retina in which the CDFs align closely with the normal distribution. On the right is a horizontal section from a TgP347L rabbit. The CDFs from 4 × 4 μm regions of those Müller cells result in widely varying CDFs that coincide with the normal distribution only in rare cases.

are buried beneath layers of other Müller cell processes and any transport of taurine from the subretinal space may vary across Müller cells. The varied levels of glutathione is consistent with previous and ongoing studies of retinal degeneration and injury in multiple models and is also found in human RP (Marc et al., 2007, 2008; Jones et al., 2016a, Jones et al., 2016b). Glutathione increase in Müller cells is likely associated with oxidative stress and one of the multiple pathways glutamate is metabolized by in the absence of GS. This however, cannot account for the total concentration of glutamate being metabolized. The continued variation of protein and small molecules demonstrates that remodeled Müller cells do not correlate their metabolomes with their neighbors.

These observations illustrate and quantify chaotic metabolic variations across Müller cells in the degenerating retina. Clearly, Müller cells have the capacity to independently respond variably to retinal stress, driving wide deviation from the robust, precise metabolic profile of the Müller cell cohort in healthy retina. The ability to deviate so widely from healthy Müller cells without showing signs of Müller cell death raises the intriguing question of what maintains the homogeneity of Müller cells in the non-pathologic state? Also, once metabolic chaos is initiated, can we reverse it and restore Müller cells to a uniform support network? The understanding of these fundamental questions will be essential to the development of robust therapeutic interventions for retinal degeneration since a lack of consistent metabolic support by Müller cells will make sustainable neurotransmission unlikely.

Acknowledgements:

Supported by: EY015128 (RM), NIH EY02576 (RM), EY014800 Vision Core, an unrestricted grant from Research to Prevent Blindness to the Moran Eye Center; Edward N. and Della L. Thome Memorial Foundation grant for Age-Related Macular Degeneration Research (BWJ), a Research to Prevent Blindness Career Development Award (BWJ), Moran Eye Center Tiger Team Translational Medicine Award (BWJ).

References

Aguirre, G., 1978. Retinal degenerations in the dog. I. Rod dysplasia. Exp. Eye Res. 26, 233–253.
Anderson, J.R., Jones, B.W., Watt, C.B., Shaw, M.V., Yang, J.H., Demill, D.,

Lauritzen, J.S., Lin, Y., Rapp, K.D., Mastronarde, D., Koshevoy, P., Grimm, B., Tasdizen, T., Whitaker, R., Marc, R.E., 2011. Exploring the retinal connectome. Mol. Vis. 17, 355–379.
Anderson, J.R., Jones, B.W., Yang, J.H., Shaw, M.V., Watt, C.B., Koshevoy, P., Spaltenstein, J., Jurrus, E., Kannan, U.V., Whitaker, R.T., Mastronarde, D., Tasdizen, T., Marc, R.E., 2009. A computational framework for ultrastructural mapping of neural circuitry. PLoS Biol. 7, e1000074.
Barnett, K.C., Curtis, R., 1985. Autosomal dominant progressive retinal atrophy in Abyssinian cats. J. Hered. 76, 168–170.
Bignami, A., Dahl, D., 1979. The radial glia of Müller in the rat retina and their response to injury. An immunofluorescence study with antibodies to the glial fibrillary acidic (GFA) protein. Exp. Eye Res. 28, 63–69.
Bourne, M.C., Campbell, D.A., Tansley, K., 1938. Hereditary degeneration of the rat retina. Br. J. Ophthalmol. 22, 613–623.
Bringmann, A., Grosche, A., Pannicke, T., Reichenbach, A., 2013. GABA and glutamate uptake and metabolism in retinal glial (Muller) cells. Front. Endocrinol. 4, 48.
Brockerhoff, S.E., Hurley, J.B., Janssen-Bienhold, U., Neuhauss, S.C., Driever, W., Dowling, J.E., 1995. A behavioral screen for isolating zebrafish mutants with visual system defects. Proc. Natl. Acad. Sci. U. S. A. 92, 10545–10549.
Chader, G.J., 2002. Animal models in research on retinal degenerations: past progress and future hope. Vis. Res. 42, 393–399.
Chang, B., Hawes, N.L., Hurd, R.E., Davisson, M.T., Nusinowitz, S., Heckenlively, J.R., 2002. Retinal degeneration mutants in the mouse. Vis. Res. 42, 517–525.
Chow, C.Y., Kelsey, K.J., Wolfner, M.F., Clark, A.G., 2016. Candidate genetic modifiers of retinitis pigmentosa identified by exploiting natural variation in Drosophila. Hum. Mol. Genet. 25 (4), 651–659.
Crawford, J.R., Garthwaite, P.H., 2012. Single-case research in neuropsychology: a comparison of five forms of t-test for comparing a case to controls. Cortex 48, 1009–1016 a journal devoted to the study of the nervous system and behavior.
Crawford, J.R., Howell, D.C., 1998. Comparing an individual's test score against norms derived from small samples. Clin. Neuropsychol. 12, 482–486.
Dreher, Z., Robinson, S.R., Distler, C., 1992. Müller cells in vascular and avascular retinae: a survey of seven mammals. J. Comp. Neurol. 323, 59–80.
Erickson, P.A., Fisher, S.K., Guerin, C.J., Anderson, D.H., Kaska, D.D., 1987. Glial fibrillary acidic protein increases in Muller cells after retinal detachment. Exp. Eye Res. 44, 37–48.
Fisher, S.K., Lewis, G.P., 2003. Muller cell and neuronal remodeling in retinal detachment and reattachment and their potential consequences for visual recovery: a review and reconsideration of recent data. Vis. Res. 43, 887–897.
Griciuc, A., Aron, L., Ueffing, M., 2012. Looking into eyes: rhodopsin pathologies in Drosophila. Adv. Exp. Med. Biol. 723, 415–423.
Han, J., Dinculescu, A., Dai, X., Du, W., Smith, W.C., Pang, J., 2013. Review: the history and role of naturally occurring mouse models with Pde6b mutations. Mol. Vis. 19, 2579–2589.
Hurley, J.B., Lindsay, K.J., Du, J., 2015. Glucose, lactate, and shuttling of metabolites in vertebrate retinas. J. Neurosci. Res. 93, 1079–1092.
Jones, B.W., Kondo, M., Terasaki, H., Lin, Y., McCall, M., Marc, R.E., 2012. Retinal remodeling. Jpn. J. Ophthalmol. 56, 289–306.
Jones, B.W., Kondo, M., Terasaki, H., Watt, C.B., Rapp, K., Anderson, J., Lin, Y., Shaw, M.V., Yang, J.H., Marc, R.E., 2011. Retinal remodeling in the Tg P347L rabbit, a large-eye model of retinal degeneration. J. Comp. Neurol. 519, 2713–2733.
Jones, B.W., Marc, R.E., 2005. Retinal remodeling during retinal degeneration. Exp. Eye Res. 81, 123–137.
Jones, B.W., Watt, C.B., Frederick, J.M., Baehr, W., Chen, C.K., Levine, E.M., Milam, A.H., Lavail, M.M., Marc, R.E., 2003. Retinal remodeling triggered by photoreceptor degenerations. J. Comp. Neurol. 464, 1–16.
Jones, B.W., Watt, C.B., Marc, R.E., 2005. Retinal remodeling. Clin. Exp. Optom. 88, 282–291.
Jones, B.W., Pfeiffer, R.L., Ferrell, W.D., Watt, C.B., Marmor, M., Marc, R.E., 2016a. Retinal remodeling in human retinitis pigmentosa. Exp. Eye Res. 150, 149–165. http://www.ncbi.nlm.nih.gov/pubmed/27020758.
Jones, B.W., Pfeiffer, R.L., Ferrell, W.D., Watt, C.B., Tucker, J.F., Marc, R.E., 2016b. Retinal remodeling and metabolic alterations in human AMD. Front. Cell. Neurosci. (in press) http://journal.frontiersin.org/article/10.3389/fncel.2016.00103/full.
Kalloniatis, M., Fletcher, E.L., 1993. Immunocytochemical localization of the amino acid neurotransmitters in the chicken retina. J. Comp. Neurol. 336, 174–193.
Kalloniatis, M., Marc, R.E., Murry, R.F., 1996. Amino acid signatures in the primate retina. J. Neurosci. Off. J. Soc. Neurosci. 16, 6807–6829.
Keeler, C.E., 1924. The inheritance of a retinal abnormality in white mice. Proc. Natl. Acad. Sci. U. S. A. 10, 329–333.
Kolb, H., Gouras, P., 1974. Electron microscopic observations of human retinitis pigmentosa, dominantly inherited. Investig. Ophthalmol. 13, 487–498.
Kondo, M., Sakai, T., Komeima, K., Kurimoto, Y., Ueno, S., Nishizawa, Y., Usukura, J., Fujikado, T., Tano, Y., Terasaki, H., 2009. Generation of a transgenic rabbit model of retinal degeneration. Investig. Ophthalmol. Vis. Sci. 50, 1371–1377.
Luna, G., Lewis, G.P., Banna, C.D., Skalli, O., Fisher, S.K., 2010. Expression profiles of nestin and synemin in reactive astrocytes and Müller cells following retinal injury: a comparison with glial fibrillar acidic protein and vimentin. Mol. Vis. 16, 2511–2523.
Marc, R., Pfeiffer, R., Jones, B., 2014. Retinal prosthetics, optogenetics, and chemical photoswitches. ACS Chem. Neurosci. 5, 895–901.
Marc, R.E., 1992. The structure of GABAergic circuits in ectotherm retinas. In: Mize, R., Marc, R.E., Sillito, A. (Eds.), GABA in the Retina and Central Visual System. Elsevier, Amsterdam, pp. 61–92.
Marc, R.E., 1999. Mapping glutamatergic drive in the vertebrate retina with a channel-permeant organic cation. J. Comp. Neurol. 407, 47–64.
Marc, R.E., 2004. Retinal neurotransmitters. In: Chalupa, L.M., Werner, J. (Eds.), The Visual Neurosciences. MIT Press, Cambridge MA, pp. 315–330.
Marc, R.E., Cameron, D., 2001. A molecular phenotype atlas of the zebrafish retina. J. Neurocytol. 30, 593–654.
Marc, R.E., Jones, B.W., 2002. Molecular phenotyping of retinal ganglion cells. J. Neurosci. Off. J. Soc. Neurosci. 22, 413–427.
Marc, R.E., Jones, B.W., 2003. Retinal remodeling in inherited photoreceptor degenerations. Mol. Neurobiol. 28, 139–147.
Marc, R.E., Jones, B.W., Anderson, J.R., Kinard, K., Marshak, D.W., Wilson, J.H., Wensel, T., Lucas, R.J., 2007. Neural reprogramming in retinal degeneration. Investig. Ophthalmol. Vis. Sci. 48, 3364–3371.
Marc, R.E., Jones, B.W., Watt, C.B., Strettoi, E., 2003. Neural remodeling in retinal degeneration. Prog. Retin. Eye Res. 22, 607–655.
Marc, R.E., Jones, B.W., Watt, C.B., Vazquez-Chona, F., Vaughan, D.K., Organisciak, D.T., 2008. Extreme retinal remodeling triggered by light damage: implications for age related macular degeneration. Mol. Vis. 14, 782–806.
Marc, R.E., Murry, R.F., Basinger, S.F., 1995. Pattern recognition of amino acid signatures in retinal neurons. J. Neurosci. Off. J. Soc. Neurosci. 15, 5106–5129.
Marc, R.E., Murry, R.F., Fisher, S.K., Linberg, K.A., Lewis, G.P., 1998a. Amino acid signatures in the detached cat retina. Investig. Ophthalmol. Vis. Sci. 39, 1694–1702.
Marc, R.E., Murry, R.F., Fisher, S.K., Linberg, K.A., Lewis, G.P., Kalloniatis, M., 1998b. Amino acid signatures in the normal cat retina. Investig. Ophthalmol. Vis. Sci. 39, 1685–1693.
Marc, R.E., Wei-Ley, S., Kalloniatis, M., Raiguel, S.F., Van Haesendonck, E., 1990. Patterns of glutamate immunoreactivity in the goldfish retina. J. Neurosci. 10, 4006–4034.
McKenna, M.C., 2007. The glutamate-glutamine cycle is not stoichiometric: fates of glutamate in brain. J. Neurosci. Res. 85, 3347–3358.
McKenna, M.C., Sonnewald, U., Huang, X., Stevenson, J., Zielke, H.R., 1996. Exogenous glutamate concentration regulates the metabolic fate of glutamate in astrocytes. J. Neurochem. 66, 386–393.
Michal, G., 1999. Amino acids and derivatives. In: Biochemical Pathways: an Atlas of Biochemistry and Molecular Biology, vol. 1. John Wiley & Sons Inc., New York, pp. 46–58.
Narfstrom, K., 1983. Hereditary progressive retinal atrophy in the Abyssinian cat. J. Hered. 74, 273–276.
Newman, E.A., Frambach, D.A., Odette, L.L., 1984. Control of extracellular potassium levels by retinal glial cell K+ siphoning. Science 225, 1174–1175.
Petters, R.M., Alexander, C.A., Wells, K.D., Collins, E.B., Sommer, J.R., Blanton, M.R., Rojas, G., Hao, Y., Flowers, W.L., Banin, E., Cideciyan, A.V., Jacobson, S.G., Wong, F., 1997. Genetically engineered large animal model for studying cone photoreceptor survival and degeneration in retinitis pigmentosa. Nat. Biotechnol. 15, 965–970.
Pittler, S.J., Keeler, C.E., Sidman, R.L., Baehr, W., 1993. PCR analysis of DNA from 70-year-old sections of rodless retina demonstrates identity with the mouse rd defect. Proc. Natl. Acad. Sci. U. S. A. 90, 9616–9619.
Poitry, S., Poitry-Yamate, C., Ueberfeld, J., MacLeish, P.R., Tsacopoulos, M., 2000. Mechanisms of glutamate metabolic signaling in retinal glial (Muller) cells. J. Neurosci. Off. J. Soc. Neurosci. 20, 1809–1821.
Pow, D.V., Robinson, S.R., 1994. Glutamate in some retinal neurons is derived solely from glia. Neuroscience 60, 355–366.
Reichenbach, A., Bringmann, A., 2010. Muller cells in the healthy retina. In: Muller Cells in the Healthy and Diseased Retina. Springer Science+Business Media, LLC.
Riepe, R.E., Norenburg, M.D., 1977. Muller cell localisation of glutamine synthetase in rat retina. Nature 268, 654–655.
Roesch, K., Stadler, M.B., Cepko, C.L., 2012. Gene expression changes within Müller glial cells in retinitis pigmentosa. Mol. Vis. 18, 1197–1214.
Rowan, S., Cepko, C.L., 2004. Genetic analysis of the homeodomain transcription factor Chx10 in the retina using novel multifunctional BAC transgene mouse reporter. Dev. Biol. 271, 388–402.
Schneider, C.A., Rasband, W.S., Eliceiri, K.W., 2012. NIH image to image J: 25 years of image analysis. Nat. Methods 9, 671–675.
Semple-Rowland, S.L., Lee, N.R., 2000. Avian models of inherited retinal disease. Methods Enzymol. 316, 526–536.
Strettoi, E., Pignatelli, V., Rossi, C., Porciatti, V., Falsini, B., 2003. Remodeling of second-order neurons in the retina of rd/rd mutant mice. Vis. Res. 43, 867–877.
Strettoi, E., Porciatti, V., Falsini, B., Pignatelli, V., Rossi, C., 2002. Morphological and functional abnormalities in the inner retina of the rd/rd mouse. J. Neurosci. Off. J. Soc. Neurosci. 22, 5492–5504.
Suber, M.L., Pittler, S.J., Qin, N., Wright, G.C., Holcombe, V., Lee, R.H., Craft, C.M., Lolley, R.N., Baehr, W., Hurwitz, R.L., 1993. Irish setter dogs affected with rod/cone dysplasia contain a nonsense mutation in the rod cGMP phosphodiesterase beta-subunit gene. Proc. Natl. Acad. Sci. U. S. A. 90, 3968–3972.
Wilson, D.J., 2002. 2-deoxy-d-glucose uptake in the inner retina: an in vivo study in the normal rat and following photoreceptor degeneration. Trans. Am. Ophthalmol. Soc. 100, 353–364.